ACS Chemical Neuroscience

LETTER

pubs.acs.org/acschemicalneuroscience

Synaptosomes as a Platform for Loading Nanoparticles into Synaptic Vesicles

Kristi L. Budzinski,[†] Allyson E. Sgro,[†] Bryant S. Fujimoto,[†] Jennifer C. Gadd,[†] Noah G. Shuart,[‡] Tamir Gonen,[‡,§] Sandra M. Bajjaleih,[∥] and Daniel T. Chiu*[,†]

[†]Department of Chemistry, [‡]Department of Biochemistry Biochemistry, [§]Howard Hughes Medical Institute, and [∥]Department of Pharmacology, University of Washington, Seattle, Washington 98195-1700, United States

Supporting Information

ABSTRACT: Synaptosomes are intact, isolated nerve terminals that contain the necessary machinery to recycle synaptic vesicles via endocytosis and exocytosis upon stimulation. Here we use this property of synaptosomes to load quantum dots into synaptic vesicles. Vesicles are then isolated from the synaptosomes, providing a method to probe isolated, individual synaptic vesicles where each vesicle contains a single, encapsulated nanoparticle. This technique provided an encapsulation efficiency of ~16%; that is, ~16% of the vesicles contained a single quantum dot while the remaining vesicles were empty. The ability to load single nanoparticles into synaptic vesicles opens new opportunity for employing various nanoparticle-based sensors to study the dynamics of vesicular transporters.

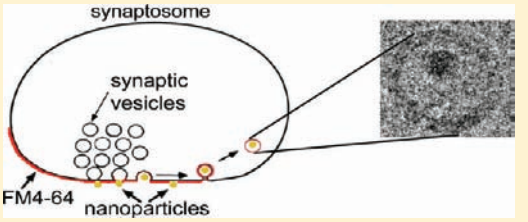

KEYWORDS: Synaptosome, quantum dots, synaptic vesicles, single molecule, nanoparticles

Synaptic vesicles are small trafficking organelles that are responsible for communication between neurons by storing and releasing neurotransmitters upon stimulation. Synaptic vesicles were first isolated from brain tissue by Whittaker et al. in 1964[1] and have been studied using mass spectrometry,[2,3] electron microscopy,[4,5] and fluorescence microscopy,[6,7] providing information about the physical properties of vesicles and neurotransmitter-loading behavior. These studies have contributed to the overall understanding of synaptic vesicles and the functions they play in neuronal communication. Unfortunately, these studies often do not probe the internal environment of the isolated vesicles. Current methods for probing the lumen of synaptic vesicles involve the use of membrane-permeable dyes such as acridine orange[8] or vesicles engineered to contain a pH sensitive GFP[9] or false fluorescent neurotransmitters, which are only available for nonspecific neurotransmitter transporters.[10] We sought to develop a technique that would allow us to probe the internal environment of synaptic vesicles using nanoparticle-based fluorescent sensors, such as those for pH, calcium, and glutamate. The ability to load synaptic vesicles with these fluorescent sensors will allow real-time readout of these important molecules with single-vesicle resolution, which in turn will enable us to produce a better understanding of the vesicular transporters that control these molecules.

We selected quantum dots as our model fluorescent sensor for a number of reasons. They are commercially available, have very well-defined absorption and emission spectra, and have well-characterized photophysical properties. Quantum dots are approximately 15 nm in diameter, which is small enough to fit inside a synaptic vesicle (40−50 nm) but too large to be transported into the vesicle or diffuse across the membrane. Quantum dots have been used previously to study neurotransmitter release in cultured neurons, revealing that quantum dots can be taken up by synaptic boutons.[11] It is difficult to isolate synaptic vesicles from cultured neurons, however, due to the limited number of cells that can be grown on a plate at one time. In order to study individual synaptic vesicles in a statistically relevant manner, we desired a technique that allows one to load and then isolate many synaptic vesicles at once. Thus, we chose to use synaptosomes as the platform for loading nanoparticles into synaptic vesicles.

Synaptosomes provide a twofold advantage for this type of experiment: (1) They contain all the machinery necessary for synaptic vesicles to go through endocytosis,[12] neurotransmitter loading,[13] and exocytosis.[14] (2) The isolation of synaptic vesicles from synaptosomes is well-characterized.[15] Synaptosomes are nerve terminals that have been separated from their axons and postsynaptic connections then reseal, retaining function that closely mimics nerve terminals in vivo.[16,17] This is achieved by homogenizing fresh brain tissue in isotonic medium, which shears denser axon terminals away from axons, then subjecting the homogenate to several specific centrifugation steps that enrich synaptic terminals based on their buoyant density.[17] Synaptosomes can be stimulated to release neurotransmitter either chemically, through the application of 30 mM (or greater) K^{+}[11] or 4-aminopyridine (4-AP),[13] or electrically, through the application of action potentials.[18] This property has allowed researchers to label synaptic vesicles with FM dyes[6,19] and membrane permeable dyes[8,14] in the study of vesicle acidification, endocytosis, and vesicle recycling. Thus, synaptosomes are a

Received: February 14, 2011
Accepted: March 8, 2011
Published: March 08, 2011

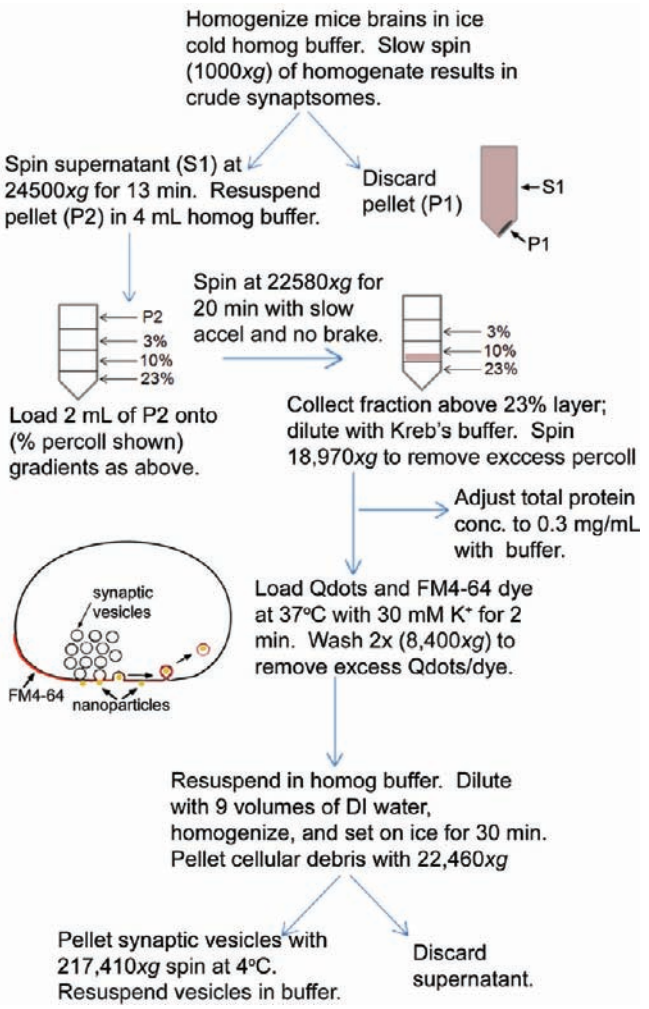

Figure 1. Purification of synaptosomes and quantum dot loading. Synaptosomes were isolated from fresh brain tissue and purified on a Percoll gradient. Quantum dots (Q605) and FM4-64 dye were loaded into synaptic vesicles by stimulating the synaptosome with an application of 30 mM K^+. The loaded synaptic vesicles were then isolated following homogenization and a two-step centrifugation procedure. Synaptic vesicles could be stored at 4 °C for about 1 week.

valid platform for loading synaptic vesicles with fluorescent markers. Here we expand the use of synaptosomes to encapsulate nanoparticles within synaptic vesicles, to promote the study of the internal makeup of isolated synaptic vesicles.

The flowchart in Figure 1 presents the method we optimized for encapsulating quantum dots in synaptic vesicles and isolation of the vesicles. The procedure has three main parts: (1) isolation of synaptosomes, (2) chemical stimulation of synaptosomes to trigger loading, and (3) synaptic vesicle isolation. Following isolation, synaptic vesicles were imaged in polydimethylsiloxane (PDMS) microwells using total internal reflection fluorescence (TIRF) microscopy (Supporting Information Figure 1).

The isolation of synaptosomes is based on methods developed by Nagy and Delgadoescueta[20] and Dunkley et al.[17] There are several important caveats for the isolation of synaptosomes for nanoparticle loading. The first is the use of a swinging bucket rotor to generate soft pellets that require less pipetting to resuspend. Care must be taken to keep as many synaptosomes intact and functional as possible. Another important step is the

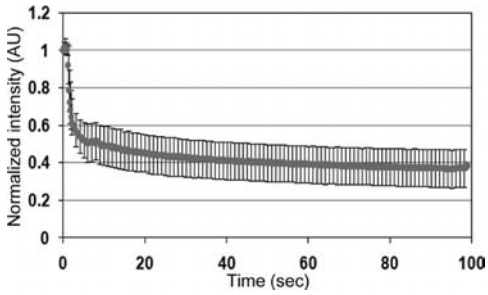

Figure 2. Destaining synaptosomes loaded with FM4-64 dye. Synaptosomes were loaded with FM4-64 dye by stimulation with 30 mM K^+. Following two washes, the synaptosomes were stimulated again with 30 mM K^+, causing the synaptic vesicles to recycle, thereby releasing the FM4-64 dye into the buffer. Imaging was performed for 100 s to capture the destaining of the synaptosomes as synaptic vesicles recycled. Fluorescence intensity was normalized to initial intensity.

use of a discontinuous Percoll gradient to purify synaptosomes from mitochondria, myelin, and synaptic and plasma membranes because the carboxyl surface groups on the quantum dots favor attachment to neuronal membranes.[11] The use of a Percoll gradient reduces the amount of extraneous neuronal membrane available for quantum dot binding. It is also important to determine the protein concentration after purifying the synaptosomes. Total protein concentration of 6−8 mg/mL is typically obtained following Percoll gradient purification, which is too high for efficient nanoparticle loading. The synaptosomes must be diluted to give a total protein concentration of approximately 0.3 mg/mL. All isolation steps were performed in isotonic medium to maintain activity.

The stimulation procedure developed to load nanoparticles is based on procedures used to load styryl dyes into synaptosomes.[19,21] Initially, we verified that the isolation procedure we optimized produced active synaptosomes by stimulating the synaptosomes in the presence of FM4-64 dye only. Synaptosomes were stimulated using a 2 min application of 30 mM K^+ Krebs-like buffer in the presence of FM4-64 dye at 37 °C. Following two wash steps, to remove excess dye, the synaptosome pellet was resuspended in Krebs-like buffer, placed in a PDMS microwell, and stimulated a second time with a second application of 30 mM K^+ Krebs-like buffer. Figure 2 shows a ∼70% decrease in fluorescence intensity following the second stimulation with high K^+ buffer, which is consistent with FM dye destaining resulting from a K^+ challenge.[22] We applied this isolation and loading method to the loading of nanoparticles into synaptic vesicles.

To confirm that synaptic vesicles were taking up nanoparticles using the synaptosome loading procedure described here, FM4-64 dye was loaded simultaneously with Q605 quantum dots. Synaptosomes were stimulated with 30 mM K^+ in the presence of FM4-64 and Q605, washed, and then ruptured to release the synaptic vesicles. Isolated synaptic vesicles were placed in a PDMS microwell and imaged using TIRF microscopy. Synaptic vesicles were initially identified by fluorescence of FM4-64 dye, shown as red puncta in panel 1, Figure 3. In a separate channel, Q605 puncta were identified (green puncta) as shown in panel 2, Figure 3. Numerous FM4-64 spots were seen when synaptic vesicles were stimulated in the presence of 30 mM K^+ (Figure 3a), indicating that synaptic vesicles were recycled in the synaptosome following stimulation. In the absence of K^+

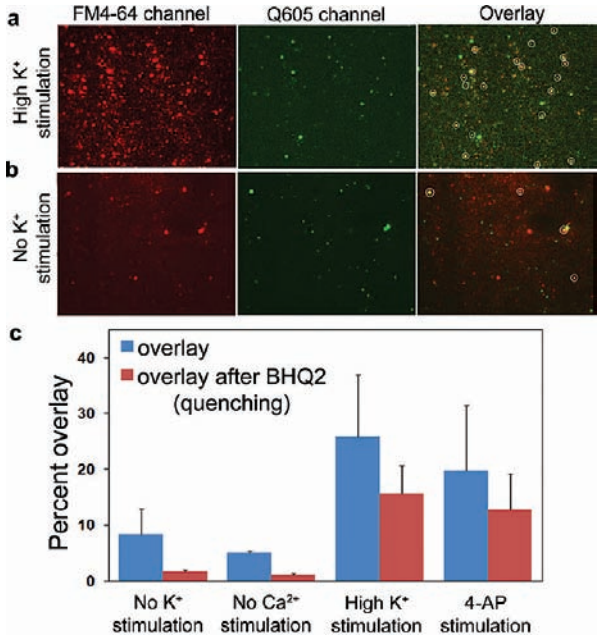

Figure 3. Overlay of FM4-64 dye and Q605 in isolated synaptic vesicles. (a,b) The left panel shows synaptic vesicles labeled with FM4-64 dye, the middle panel shows the same vesicles labeled with Q605, and the right panel shows the overlay between the two channels. (a) For synaptic vesicles isolated from synaptosomes stimulated with 30 mM K^+, 20−30% of synaptic vesicle population identified by FM4-64 (red channel) overlaid with Q605 spots (green channel). (b) Control sample showing synaptic vesicles isolated from synaptosomes stimulated with Krebs-like buffer (4 mM K^+), where <10% of vesicles identified by FM4-64 overlaid with Q605 spots. (c) Bar graph showing percentage of overlay for vesicles before (blue) and after (red) BHQ2 quenching treatment under different stimulation conditions. No K^+ stimulation (same condition as in panel b), no Ca2+ stimulation (done using buffer without CaCl2), high K^+ stimulation (same condition as in panel a), 4-AP stimulation (done using1 mM 4-aminopyridine). Error bars represent SEM of overlay percentage.

stimulation (Figure 3b), few FM4-64 spots were detected; these spots were probably the result of spontaneous recycling synaptic vesicles.[23] The third column in Figure 3 represents the overlay between the FM4-64 channel and the Q605 channel. The histogram in Figure 3c shows the percent of FM4-64-labeled vesicles that were matched to a Q605 spot under various loading conditions. For vesicles loaded using high K^+ stimulation, 25.8 ± 11.1% (Figure 3c) of the vesicles identified by FM4-64 overlay with a Q605 spot as determined by an in-house developed MATLAB program that analyzes two color images[24] and matches puncta from one image to puncta in the second image. The percentage of vesicles loaded with quantum dots achieved using synaptosomes agrees well with the percentage of loading achieved in cultured neurons,[11] confirming that synaptosomes are a viable platform for loading synaptic vesicles with nanoparticles.

Stimulation using 4-aminopyridine (4-AP) was also tested to determine if one stimulation method was superior for nanoparticle loading. Applications of high K^+ directly depolarize the plasma membrane by voltage clamping that produces localized increases in Ca^{2+} while 4-AP blocks presynaptic K^+ channels, which results in repetitive membrane depolarizations, thereby creating localized Ca^{2+} increases. As shown in the histogram in Figure 3c, both high K^+ and 4-AP stimulation produced overlay

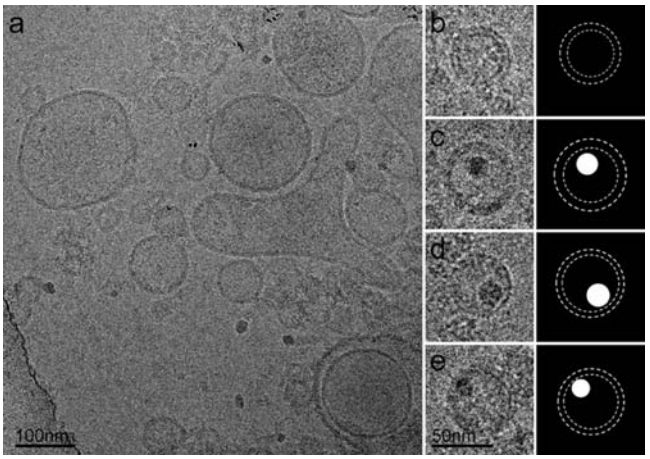

Figure 4. Cryo-electron microscopy images of isolated synaptic vesicles loaded with quantum dots. (a) Representative overview of isolated synaptic vesicle images collected using cryoEM. The sample contained both synaptic vesicles ranging in size from ∼30 to 60 nm and larger membranous structures ranging in size from ∼80 to 150 nm. The larger structures are probably derived from synaptosomal plasma membrane contaminants. (b) Empty synaptic vesicle ∼50 nm in diameter. (c−e) Synaptic vesicles containing a quantum dot. Average vesicle size is 55 nm with average quantum dot size of 16 nm. Black and white images are shown for clarity. Dashed white line represents synaptic vesicle membrane, and white spot represents quantum dot.

between FM4-64-labeled synaptic vesicles and quantum dots. Stimulation with high K^+ produced the greatest effect, with an overlay percent of 25.8 ± 11.1% compared to 19.8 ± 11.7% overlay for vesicles loaded by application of 4-AP. To verify that the quantum dots matched to synaptic vesicles (i.e., overlaid with FM4-64) were truly encapsulated within synaptic vesicles, the loading experiment was performed in the absence of high K^+ stimulation and, separately, in the absence of Ca^{2+}. Without K^+ during stimulation, the overlay between vesicles identified by FM4-64 and Q605 decreased to 8.4 ± 4.5% (Figure 3c) which suggested that spontaneous recycling vesicles may be loading nanoparticles. Since the fusion/exocytosis step requires the presence of a Ca^{2+} spike,[25] we removed Ca^{2+} from the Krebs-like buffer and added 1 mM EGTA to the synaptosomes before loading. Only 5.0 ± 0.3% of vesicles (identified by FM4-64) matched a quantum dot spot when synaptosomes were stimulated in the absence of Ca^{2+}. It should be noted that the number of vesicles labeled with FM4-64 was significantly lower when synaptosomes were stimulated in the absence of high K^+ or Ca^{2+}. For stimulated synaptosomes, our MATLAB program routinely identified >1000 puncta as valid synaptic vesicle spots; without high K^+ or Ca^{2+}, the number of puncta identified as valid synaptic vesicle spots decreased to <200.

For visual confirmation that the quantum dots were encapsulated into synaptic vesicles and not nonspecifically associated with vesicles or membrane contaminants, we visualized the quantum dot loaded synaptic vesicles using cryogenic electron microscopy (cryoEM). Samples of isolated synaptic vesicles were plunge-frozen in vitrified ice and imaged without further manipulation. Figure 4a shows a representative image of the synaptic vesicle sample. Many synaptic vesicles with diameters ranging from 30 to 60 nm were seen in addition to larger membranous structures that ranged in size from 80 to 150 nm. These larger structures probably correspond to synaptosomal plasma membrane,

myelin, or endoplasmic reticulum plasma membrane contaminants, which are typically found in synaptic vesicle preparations.[26] An empty, isolated synaptic vesicle is shown in Figure 4b for comparison on the same length scale as the quantum dot loaded synaptic vesicles shown in Figure 4c−e. Loaded synaptic vesicles ranged in diameter from 51 to 58 nm, and the quantum dots ranged in diameter from 14 to 19 nm. The quantum dots seemed to reside off-center in the synaptic vesicles, consistent with the images collected by Zhang et al. of synaptic vesicles containing quantum dots in neuronal cells.[11] Unlike fluorescence imaging using FM4-64 where we can selectively visualize synaptic vesicles only, cryoEM is nonselective and images all membranous structures in our sample. As a result, quantum dot containing vesicles were tedious to detect using cryoEM imaging, with approximately 1−2% of the total membraneous structures imaged containing a quantum dot.

Similar numbers of quantum dot spots appeared in both the high K^+ stimulation (Figure 3a) and no K^+ stimulation (Figure 3b) panels, and extraneous quantum dots can be seen in the cryo-electron micrographs (Figure 4). This suggested that nonencapsulated quantum dots are not fully removed during the wash steps and, possibly, that the quantum dots are nonspecifically associated with synaptic vesicles or contaminating neuronal membranes. We applied our MATLAB program that analyzes two color images[24] to determine the percentage of the quantum dot population that matched (or overlaid) with synaptic vesicle spots. We found that 60−70% of the quantum dot population overlaid with an FM4-64-labeled vesicle (data not shown); it should be noted that this percentage is different from the percent of FM4-64-labeled vesicles that overlay with quantum dots as discussed in preceding paragraphs and reported in the figures. Thus, extraneous quantum dots are present in the sample following synaptic vesicle isolation. The quantum dots utilized in these experiments have a polymer coating that terminates with carboxyl groups to enhance their biocompatibility, which favor attachments to neuronal membranes, making it difficult to remove nonencapsulated quantum dots by washing. The procedure includes two wash steps to remove excess quantum dots and FM4-64 dye, and as each wash requires a centrifugation and resuspension that can damage the syanptosomes, we did not want to increase the number of wash steps. Thus, it was necessary to develop another method for distinguishing nonencapsulated quantum dots from those that are encapsulated in synaptic vesicles.

We desired a method to distinguish encapsulated from nonencapsulated quantum dots that would not reduce the synaptic vesicle concentration or alter their ability to load neurotransmitter. We opted to quench nonencapsulated quantum dots on the coverglass surface rather than add another separation step. Black hole quenchers are dye molecules that have no native emission but quench other emitters through FRET or static quenching. BHQ2-NH_2 is a black hole quencher with a broad absorption spectrum (see Supporting Information Figure 2) that centers around 600 nm, thus matching the emission peak of the quantum dot chosen for these experiments, Q605. FM4-64 is not affected by the addition of BHQ2, as its emission peak is centered at 750 nm. Quantum dot quenching by BHQ2 seems to occur via static quenching as the reaction is irreversible and is distance dependent. Static quenching occurs at <2 nm; thus, quantum dots encapsulated within synaptic vesicles will not be quenched by the addition of BHQ2. Figure 5a shows the overlay images of synaptic vesicles loaded by high K^+ stimulation before and after

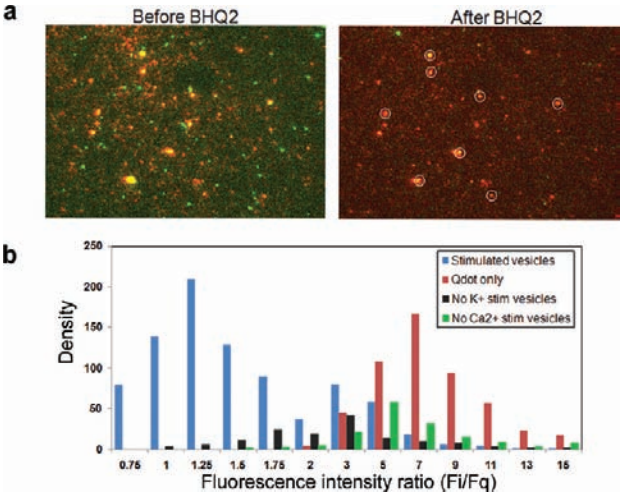

Figure 5. Synaptic vesicle overlay after treatment with BHQ2-NH2. (a) Images showing overlay between FM4-64 and Q605 channels for 30 mM K^+ loaded synaptic vesicles before (left panel) treatment with BHQ2-NH2 and after (right panel) treatment with 10 M BHQ2-NH2. (b) Fluorescent intensity ratio [initial intensity (F_i)/intensity after quenching (F_q)] of Q605 labeled vesicles after treatment with BHQ2-NH2. Stimulated synaptic vesicles (blue bars) exhibit two populations of fluorescence intensity ratio. One population has a fluorescence intensity ratio centered at 1.25, showing that BHQ2-NH2 treatment did not alter the fluorescence intensity. The other population has a ratio centered at 5 indicating that this population corresponded to Q605 quantum dots that were attached to the vesicle surface. Quantum dots placed on the glass surface and treated with BHQ2-NH2 (red bars) have a ratio centered at 7 confirming that application of BHQ2-NH2 quenches quantum dot fluorescence. In the absence of stimulation (no K^+ stim vesicles; black bars), BHQ2-NH2 quenched 70% of the quantum dots, and in the absence of Ca^{2+} (green bars) BHQ2-NH2 quenched 98% of the quantum dots.

the application of BHQ2. Before BHQ2, 25.8% of vesicles (KCl stimulation) matched a quantum dot, and after BHQ2, 15.6 ± 5.1% of vesicles matched a quantum dot (see Figure 3c). The decrease in the percentage of overlay is expected to be due to the presence of broken synaptic vesicles whose interiors will be exposed to BHQ2 and nonencapsulated quantum dots that are externally associated with synaptic vesicles due to their carboxyl coating.[11] BHQ2 quenching identifies quantum dots associated with damaged vesicles or vesicle exteriors.

The BHQ2 assay was further validated by comparing the final intensity of quantum dot puncta after BHQ2 treatment to their initial intensity (eq 1). Here F_i is the initial intensity of Q605 region of interest (ROI) selected in Metamorph, and F_q is the intensity of the same Q605 ROI following BHQ2 quenching.

$$\text{intensity ratio} = F_i/F_q \quad (1)$$

This analysis reveals encapsulated quantum dots because their intensity ratio does not change upon BHQ2 addition. Figure 5b presents a histogram of intensity ratios obtained for quantum dots under varying conditions. Quantum dots on the coverglass surface had an intensity ratio centered at 7; none had an intensity ratio of 1, showing that all quantum dots on the coverglass surface were quenched by BHQ2 as anticipated. The histogram of quantum dot intensity ratios for synaptic vesicle samples stimulated with either 4-AP or high K^+ revealed two populations after BHQ2 treatment. One population had an intensity ratio centered

at 1.25 corresponding to encapsulated quantum dots. Encapsulated quantum dots account for 75% of the quantum dots analyzed (853 spots). A second population had an intensity ratio centered at 5 corresponding to nonencapsulated quantum dots.

In the absence of stimulation, the distribution of quantum dot intensity ratios shifted to larger values, indicating the existence of nonencapsulated quantum dots, although approximately 30% of this population (141 spots) still had an intensity ratio corresponding to encapsulated quantum dots. This population probably corresponds to spontaneously recycling synaptic vesicles that can encapsulate quantum dots. Removing Ca^{2+} from the sample shifted the intensity ratios to even higher values, leaving only 2% of the population (154 spots) unquenched. Thus, encapsulated quantum dots can be identified, on chip, from nonencapsulated quantum dots that are quenched by BHQ2. This experiment also confirms quantum dots were successfully loaded into the interior of synaptic vesicles.

In summary, we have developed a method for loading nanoparticles into synaptic vesicles that can then be isolated for further study. Quantum dots can be loaded using either 30 mM K^+ stimulation or 1 mM 4-AP stimulation, with high K^+ stimulation resulting in a slightly higher percentage of vesicles ($25.8 \pm 11.1\%$ vs $19.8 \pm 11.7\%$) being matched to a quantum dot spot. It has been suggested that there are two modes of synaptic vesicle recycling: full fusion where the vesicle fuses completely with the plasma membrane, and kiss-and-run where the vesicle fuses transiently with plasma membrane and releases its contents through a small (1−5 nm) fusion pore.[27,28] Previous work with synaptosomes has suggested that high K^+ stimulation induces full fusion whereas high concentrations of 4-AP (>0.3 mM) can stimulate both full fusion and partial (kiss-and-run) fusion.[19] If high K^+ application stimulates full fusion only, this would explain the larger percentage of synaptic vesicles containing a quantum dot after synaptosomes were stimulated with high K^+; quantum dots are too large to enter through the putative fusion pore (1−5 nm) formed during kiss-and-run. For future single-vesicle studies, we have devised an effective assay using black hole quenchers to distinguish those vesicles with encapsulated fluorescent nanoparticles from those with only nonspecifically associated nanoparticles. From this assay, we were able to determine that approximately 16% of the recycling synaptic vesicles, as visualized with FM4-64, encapsulate a quantum dot. As the field of nanoparticles continues to grow and new sensors are being developed,[29,30] we anticipate this technique will allow information regarding the makeup of the synaptic vesicle interior to be gathered and the dynamics of vesicular transporters to be probed with high resolution.

■ ASSOCIATED CONTENT

Supporting Information. Detailed descriptions of experimental procedures. This material is available free of charge via the Internet at http://pubs.acs.org.

■ AUTHOR INFORMATION

Corresponding Author

*E-mail: chiu@chem.washington.edu.

Author Contributions

K.L.B. designed the study, performed loading and quenching experiments, and wrote the manuscript. A.E.S. provided experimental design consultation and animal husbandry. B.S.F. wrote the MATLAB program and provided data analysis input. J.C.G. helped with imaging experiments. T.G. and N.G.S. performed cryoEM experiments and prepared corresponding figures. S.M.B. provided lab space, equipment, animals, and input into the synaptosome preparation. D.T.C. supervised and provided input to the overall project.

Funding Sources

We gratefully acknowledge support of this work by the National Institutes of Health (NS062725). We thank the Murdock Charitable Trust and the Washington Research Foundation for generous support of our electron cryomicroscopy laboratory. T. G. is a Howard Hughes Medical Institute Early Career Scientist.

■ REFERENCES

(1) Whittaker, V. P., Michaelson, I. A., and Kirkland, R. J. (1964) Separation of Synaptic Vesicles from Nerve-Ending Particles (Synaptosomes). *Biochem. J. 90*, 293–305.

(2) Takamori, S., Holt, M., Stenius, K., Lemke, E. A., Gronborg, M., Riedel, D., Urlaub, H., Schenck, S., Brugger, B., Ringler, P., Muller, S. A., Rammner, B., Grater, F., Hub, J. S., De Groot, B. L., Mieskes, G., Moriyama, Y., Klingauf, J., Grubmuller, H., Heuser, J., Wieland, F., and Jahn, R. (2006) Molecular anatomy of a trafficking organelle. *Cell 127*, 831–846.

(3) Coughenour, H. D., Spaulding, R. S., and Thompson, C. M. (2004) The synaptic vesicle proteome: A comparative study in membrane protein identification. *Proteomics 4*, 3141–3155.

(4) Matteoli, M., Takei, K., Perin, M. S., Sudhof, T. C., and Decamilli, P. (1992) Exo-Endocytotic Recycling of Synaptic Vesicles in Developing Processes of Cultured Hippocampal Neurons. *J. Cell Biol. 117*, 849–861.

(5) Steyer, J. A., Horstmann, H., and Almers, W. (1997) Transport, docking and exocytosis of single secretory granules in live chromaffin cells. *Nature 388*, 474–478.

(6) Chen, X., Barg, S., and Almers, W. (2008) Release of the styryl dyes from single synaptic vesicles in hippocampal neurons. *J. Neurosci. 28*, 1894–1903.

(7) Budzinski, K. L., Allen, R. W., Fujimoto, B. S., Kensel-Hammes, P., Belnap, D. M., Bajjalieh, S. M., and Chiu, D. T. (2009) Large Structural Change in Isolated Synaptic Vesicles upon Loading with Neurotransmitter. *Biophys. J. 97*, 2577–2584.

(8) Zoccarato, F., Cavallini, L., and Alexandre, A. (1999) The pH-sensitive dye acridine orange as a tool to monitor exocytosis/endocytosis in synaptosomes. *J. Neurochem. 72*, 625–633.

(9) Li, Z. Y., Burrone, J., Tyler, W. J., Hartman, K. N., Albeanu, D. F., and Murthy, V. N. (2005) Synaptic vesicle recycling studied in transgenic mice expressing synaptopHluorin. *Proc. Natl. Acad. Sci. U.S.A. 102*, 6131–6136.

(10) Gubernator, N. G., Zhang, H., Staal, R. G. W., Mosharov, E. V., Pereira, D. B., Yue, M., Balsanek, V., Vadola, P. A., Mukherjee, B., Edwards, R. H., Sulzer, D., and Sames, D. (2009) Fluorescent False Neurotransmitters Visualize Dopamine Release from Individual Presynaptic Terminals. *Science 324*, 1441–1444.

(11) Zhang, Q., Cao, Y. Q., and Tsien, R. W. (2007) Quantum dots provide an optical signal specific to full collapse fusion of synaptic vesicles. *Proc. Natl. Acad. Sci. U.S.A. 104*, 17843–17848.

(12) Cousin, M. A., and Robinson, P. J. (2000) Ca^{2+} influx inhibits dynamin and arrests synaptic vesicle endocytosis at the active zone. *J. Neurosci. 20*, 949–957.

(13) Wheller, D. D., and Wise, W. C. (1983) A Kinetic Analysis of the Release of Acidic Amino-Acids from Rat Cortical Synaptosomes Following Pre-loading with Carbon-14 Labeled Glutamic-acid. *Neurochem. Res. 8*, 1111–1134.

(14) Melnik, V. I., Bikbulatova, L. S., Gulyaeva, N. V., and Bazyan, A. S. (2001) Synaptic vesicle acidification and exocytosis studied with

acridine orange fluorescence in rat brain synaptosomes. *Neurochem. Res. 26*, 549–554.

(15) Huttner, W. B., Schiebler, W., Greengard, P., and Decamilli, P. (1983) Synapsin-I (Protein-I), A Nerve Terminal-Specific Phosphoprotein.3. Its Association with Synaptic Vesicles Studied in a Highly Purified Synaptic Vesicle Preparation. *J. Cell Biol. 96*, 1374–1388.

(16) Whittaker, V. P. (1993) 30 Years of Synaptosome Research. *J. Neurocytol. 22*, 735–742.

(17) Dunkley, P. R., Jarvie, P. E., and Robinson, P. J. (2008) A rapid Percoll gradient procedure for preparation of synaptosomes. *Nat. Protoc. 3*, 1718–1728.

(18) Bradford, H. F. (1970) Metabolic response of synaptosomes to electrical stimulation: Release of amino acids. *Brain Res. 19*, 239–247.

(19) Cousin, M. A., and Robinson, P. J. (2000) Two mechanisms of synaptic vesicle recycling in rat brain nerve terminals. *J. Neurochem. 75*, 1645–1653.

(20) Nagy, A., and Delgadoescueta, A. V. (1984) Rapid Preparation of Synaptosomes from Mammalian Brain Using Nontoxic Isoosmotic Gradient Material (Percoll). *J. Neurochem. 43*, 1114–1123.

(21) Betz, W. J., Mao, F., and Smith, C. B. (1996) Imaging exocytosis and endocytosis. *Curr. Opin. Neurobiol. 6*, 365–371.

(22) Pyle, J. L., Kavalali, E. T., Choi, S., and Tsien, R. W. (1999) Visualization of synaptic activity in hippocampal slices with FM1-43 enabled by fluorescence quenching. *Neuron 24*, 803–808.

(23) Ryan, T., A., Reuter, H., and Smith, S. J. (1997) Optical detection of a quantal presynaptic membrane turnover. *Nature 388*, 478–482.

(24) Mutch, S. A., Kensel-Hammes, P., Gadd, J. C., Fujimoto, B. S., Allen, R. W., Schiro, P. G., Lorenz, R. M., Kuyper, C. L., Kuo, J. S., Bajjalieh, S. M., and Chiu, D. T. (2011) Protein Quantification at the Single Vesicle Level Reveals That a Subset of Synaptic Vesicle Proteins Are Trafficked with High Precision. *J. Neurosci. 31*, 1461–1470.

(25) Sudhof, T. C. (1995) The Synaptic Vesicle Cycle - A Cascacde of Protein-Protein Interactions. *Nature 375*, 645–653.

(26) Morgan, I. G., Vincendo., G, and Gombos, G. (1973) Adult Rat-brain Synaptic Vesicles.1. Isolation and Characterization. *Biochim. Biophys. Acta 320*, 671–680.

(27) Jackson, M. B., and Chapman, E. R. (2006) Fusion pores and fusion machines in Ca^{2+}-triggered exocytosis. *Annu. Rev. Biophys. Biomol. Struct. 35*, 135–160.

(28) Koenig, J. H., and Ikeda, K. (1996) Synaptic vesicles have two distinct recycling pathways. *J. Cell Biol. 135*, 797–808.

(29) Chan, Y. H., Jin, Y., Wu, C., and Chiu, D. T. (2011) Copper(II) and iron(II) ion sensing with semiconducting polymer dots. *Chem. Commun. 47*, 2820–2822.

(30) Chan, Y. H., Wu, C., Ye, F., Jin, Y., Smith, P. B., and Chiu, D. T. (2011) Development of Ultrabright Semiconducting Polymer Dots for Ratiometric pH Sensing. *Anal. Chem. 83*, 1448–1455.